Cell Reports, Volume *36*

Supplemental information

Methylation of dual-specificity phosphatase 4 controls cell differentiation

Hairui Su, Ming Jiang, Chamara Senevirathne, Srinivas Aluri, Tuo Zhang, Han Guo, Juliana Xavier-Ferrucio, Shuiling Jin, Ngoc-Tung Tran, Szu-Mam Liu, Chiao-Wang Sun, Yongxia Zhu, Qing Zhao, Yuling Chen, LouAnn Cable, Yudao Shen, Jing Liu, Cheng-Kui Qu, Xiaosi Han, Christopher A. Klug, Ravi Bhatia, Yabing Chen, Stephen D. Nimer, Y. George Zheng, Camelia Iancu-Rubin, Jian Jin, Haiteng Deng, Diane S. Krause, Jenny Xiang, Amit Verma, Minkui Luo, and Xinyang Zhao

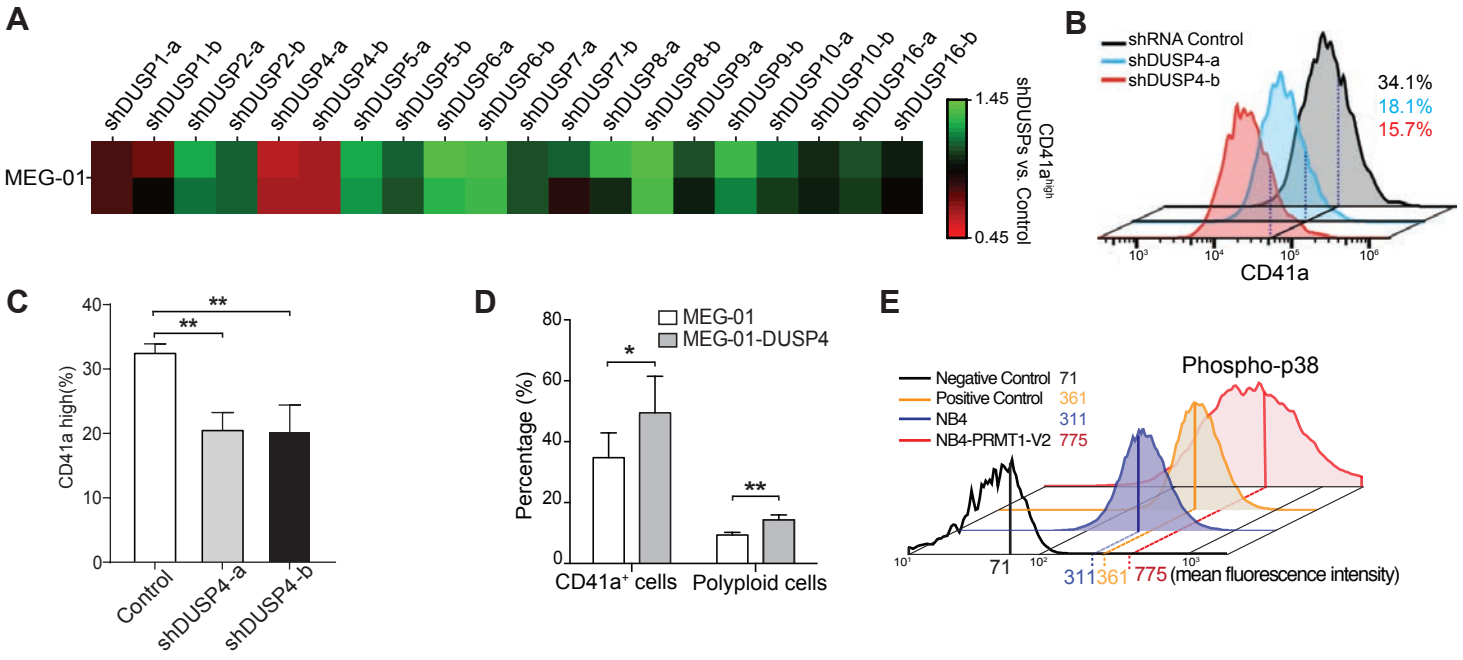

Figure S1. Requirement of DUSP4 for optimal Mk differentiation of MEG-01 cells, related to Figure 1.

(A) Heatmap of the percentages of CD41a+ cells upon knockdown of DUSPs in MEG-01 cells. MEG-01 cells were infected with lentiviruses containing a control RNA or shRNAs against DUSPs. Two shRNAs were used for each DUSP with a replicate. Percentages of CD41a+ cells in each DUSP knockdown were normalized to those of the paired control. Normalized ratios are indicated in the heatmap in color scale.

(B) and (C) Representative FACS and rigorous statistical analysis are respectively shown for the data above with 3 independent replicates (n = 3). Statistics were shown as mean ± SD, two-tailed paired t-test, **P ≤ 0.01.

(D) Analysis of Mk differentiation of MEG-01 cells upon DUSP4 overexpression. MEG-01 cells and MEG-01-DUSP4 cells were collected for FACS analysis of CD41a and DNA content (PI staining). Cells with >4N of DNA content were characterized as polyploid. Statistics were shown as mean ± SD, two-tailed paired t-test, *P≤ 0.05; **P ≤ 0.01 (n = 3, independent experiments).

(E) FACS analysis of the intracellular phospho-p38 level of parental and PRMT1-overexpressing NB4 cells. Cells were fixed by 0.4% PFA and then 4% PFA, and permeabilized by methanol for antibody staining. Negative and positive controls for NB4 cells without antibody stain and stained with anti-PE-phospho-S6K control antibody, respectively. Cells were harvested at indicated time points for western blotting. Representative plots are shown (n = 2, independent experiments).

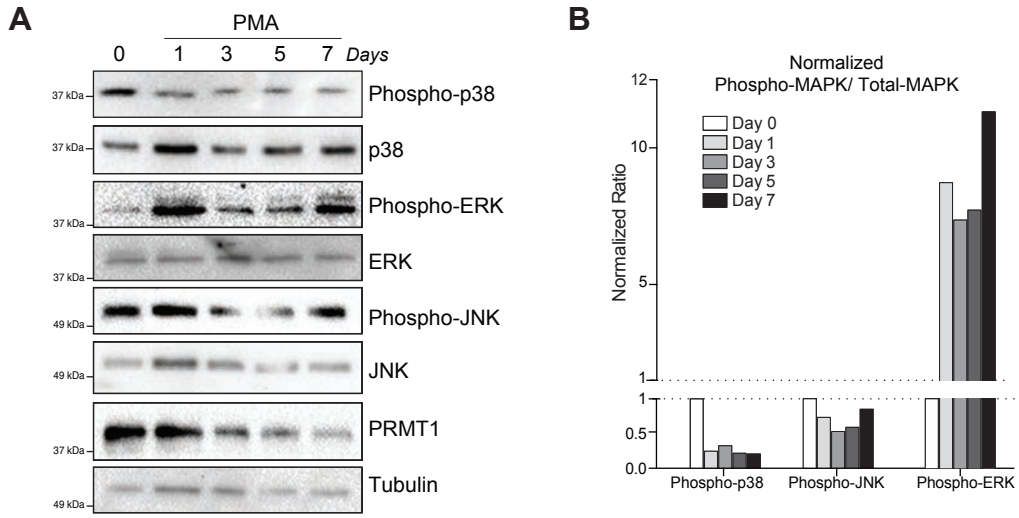

Figure S2. JNK kinase phosphorylation was modestly changed during Mk differentiation of MEG01 cells, related to Figure 3.
(A) MEG-01 cells were stimulated with PMA. The cell lysates were harvested on the indicated days for western blotting with antibodies shown the left side of blots.
(B) The ratio of band densities of activated kinases to total kinase levels.

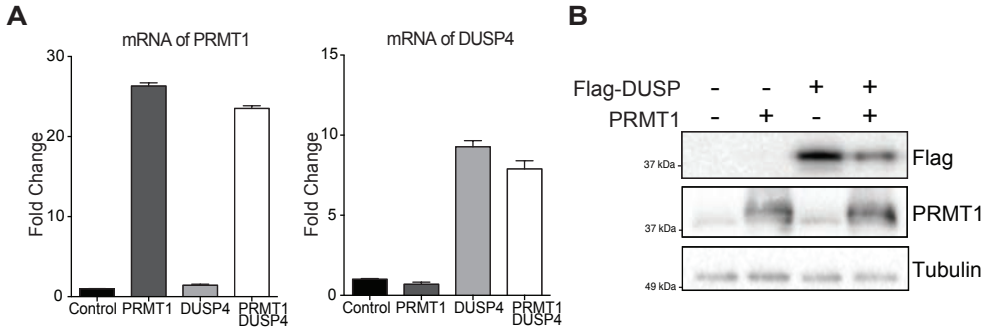

Figure S3. Verification of overexpression of DUSP4 and PRMT1 in virus-transduced CD34+ cells, Related to Figure 3F.

(A) Verification of gene expression after viral transduction. CD34+ cells were cultured in basic cytokine mix medium (IMDM, 20%BIT, SCF, FLT3L, TPO and IL-6) for two days before viral infection. Viral vectors pBGJR-DUSP4 and pTripZ-PRMT1V2 were used to express genes, and empty virus were used as controls. Three rounds of infection were performed with 12-hour gaps. Forty-eight hours post the last infection, puromycin was added to culture to select pTripZ infected cells. After 72 hours of selection, GFP+ cells (pBGJR-infected) were collected by flow cytometry. Expression of transduced genes were verified by qPCR. Representative statistics were shown as mean ± SD, two-tailed paired t-test, *P≤ 0.05; **P ≤ 0.01 (n = 2, independent experiments).

(B) Whole-cell extract of sorted cells were used for western blotting.

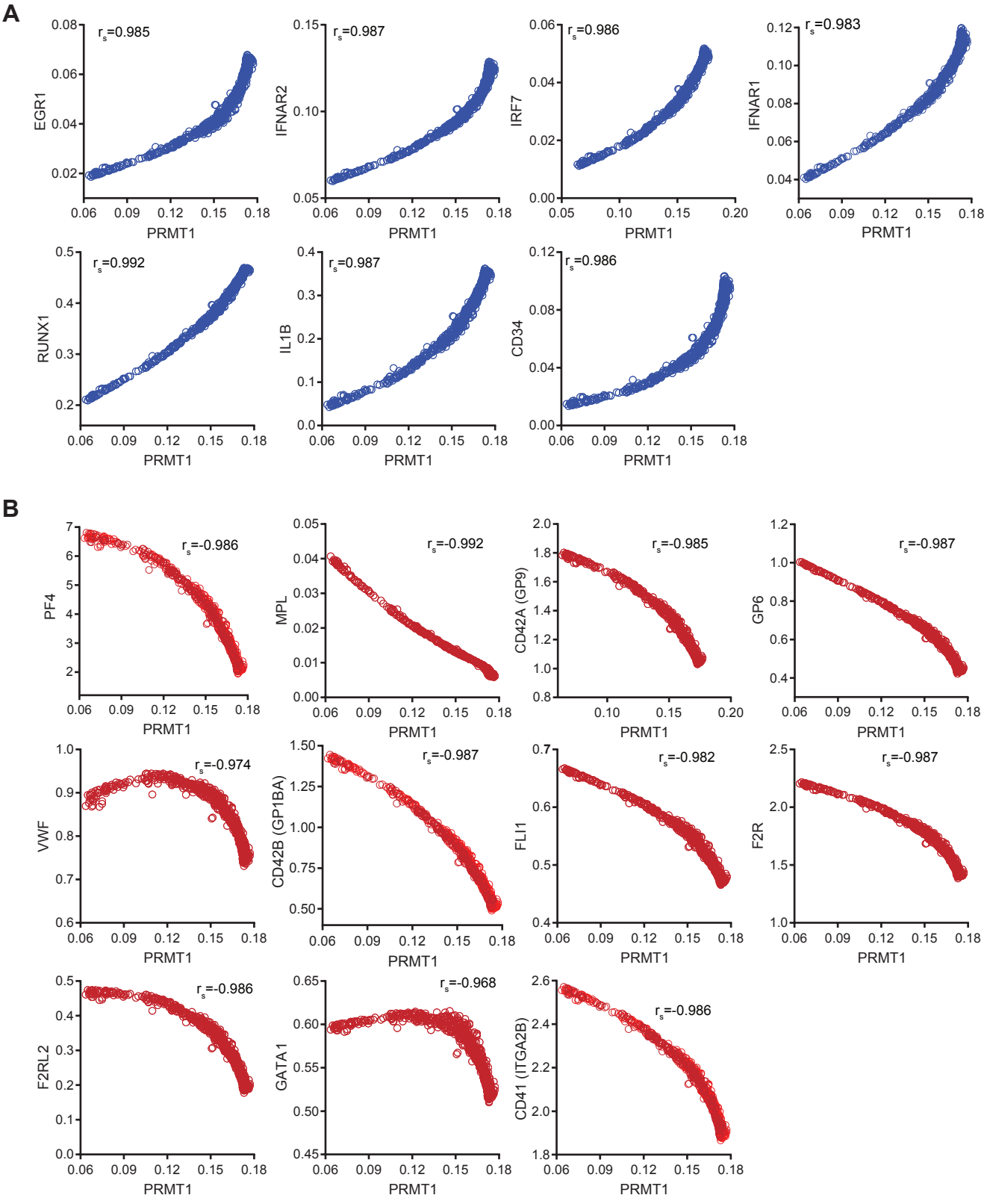

Figure S4. Single-cell RNA sequencing analysis of the Spearman correlation between PRMT1 and the transcript signature associated with Mk differentiation, Related to Figure 4E and 4G.

(A) and (B) Normalized transcripts of Mk-relevant genes negatively and positively correlated with PRMT1 in Mk-stimulated CD41a+CD42b+ cells with single-cell resolution.

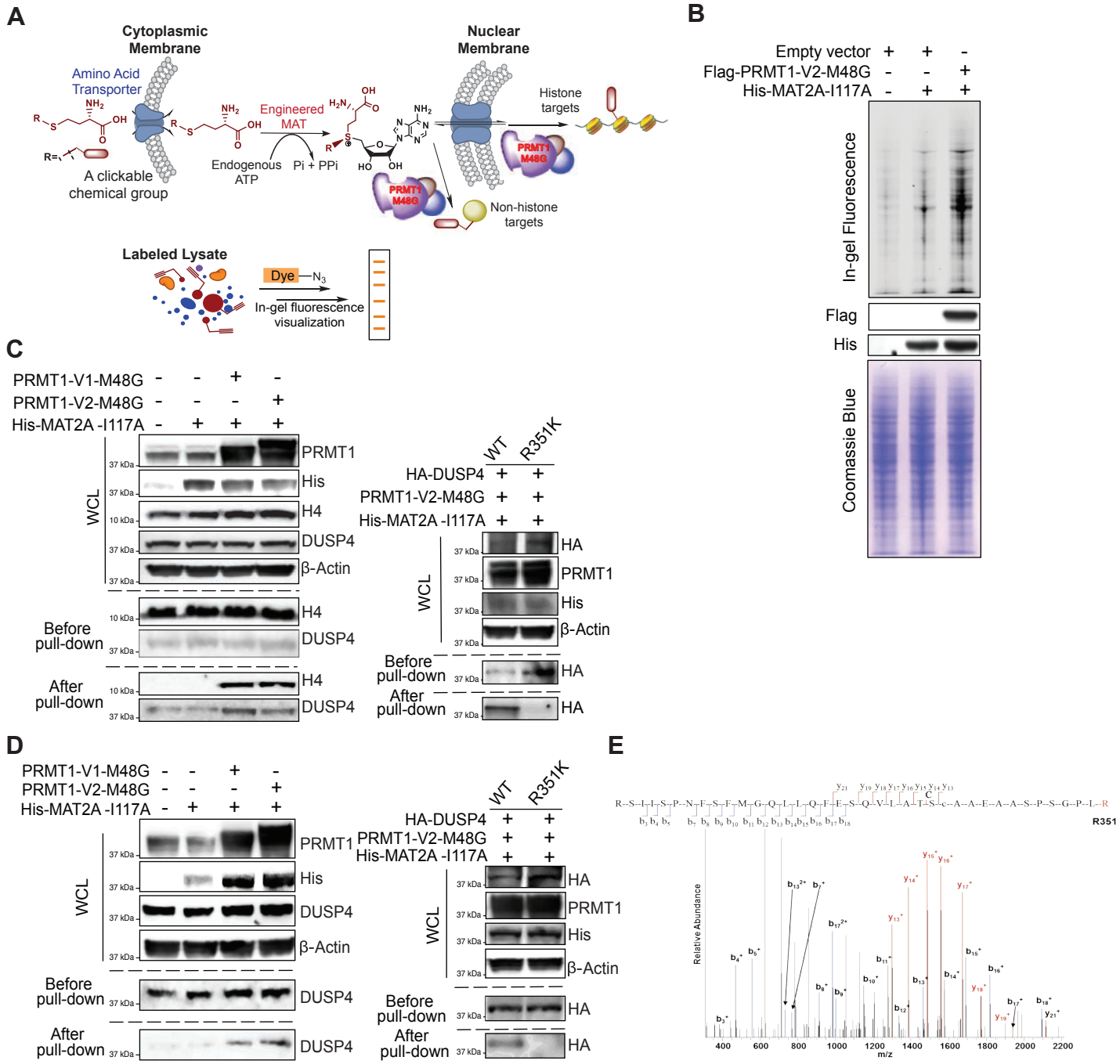

Figure S5. Further validation of DUSP4 arginine methylation by BPPM and mass spectrometry, Related to Figure 5.

(A) Schematic description of the BPPM technology coupled with in-gel fluorescence visualization. BPPM-labeled substrates were conjugated with TAMRA-dye via a click reaction, followed by electrophoresis and in-gel visualization.

(B) BPPM-revealed substrates of PRMT1 with in-gel fluorescence as readout. HEK293T cells were transfected with various combination of BPPM reagents. Their expression was confirmed by immunoblotting. The cell lysate was subject to TAMRA-dye via the click reaction, followed by in-gel fluorescence visualization. The total protein loading was shown by Coomassie Brilliant Blue staining.

(C) and (D) Revealing substrate(s) and methylation site(s) of PRMT1 with the next-generation live-cell BPPM technology. NB4 cells (C) and K562 cells (D) exposed with various combinations of BPPM reagents and DUSP4 (wild-type and R351K mutant) were treated with membrane permeable Hey-Met, which produces the SAM analogue cofactor Hey-SAM in situ, as described in Figure 5. Modified substrates were enriched by streptavidin beads and subject to western blotting. Samples before and after biotin-streptavidin pull-down were analyzed.

(E) Mass spectrometric analysis of methylated DUSP4 peptides. Recombinant DUSP4 was incubated with recombinant PRMT1 and SAM followed by SDS-PAGE separation. The DUSP4 band was digested with trypsin and subject to mass spectrum analysis. The fragment pattern was assigned as a DUSP4 peptide containing R351 methylation.

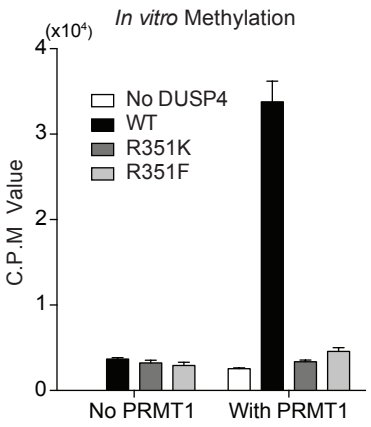

Figure S6. In vitro methylation of DUSP4 by PRMT1, Related to Figure 5. Recombinant PRMT1 was used to methylate recombinant wild-type and mutant DUSP4 protein. The PRMT1 protein and DUSP4 proteins were purified using Ni-bead via histidine tags. Scintillation counts of different reactions were performed by incubating recombinant PRMT1 and DUSP4 proteins with H3-SAM. Representative results were shown as mean ± SD (n = 2, independent experiments).

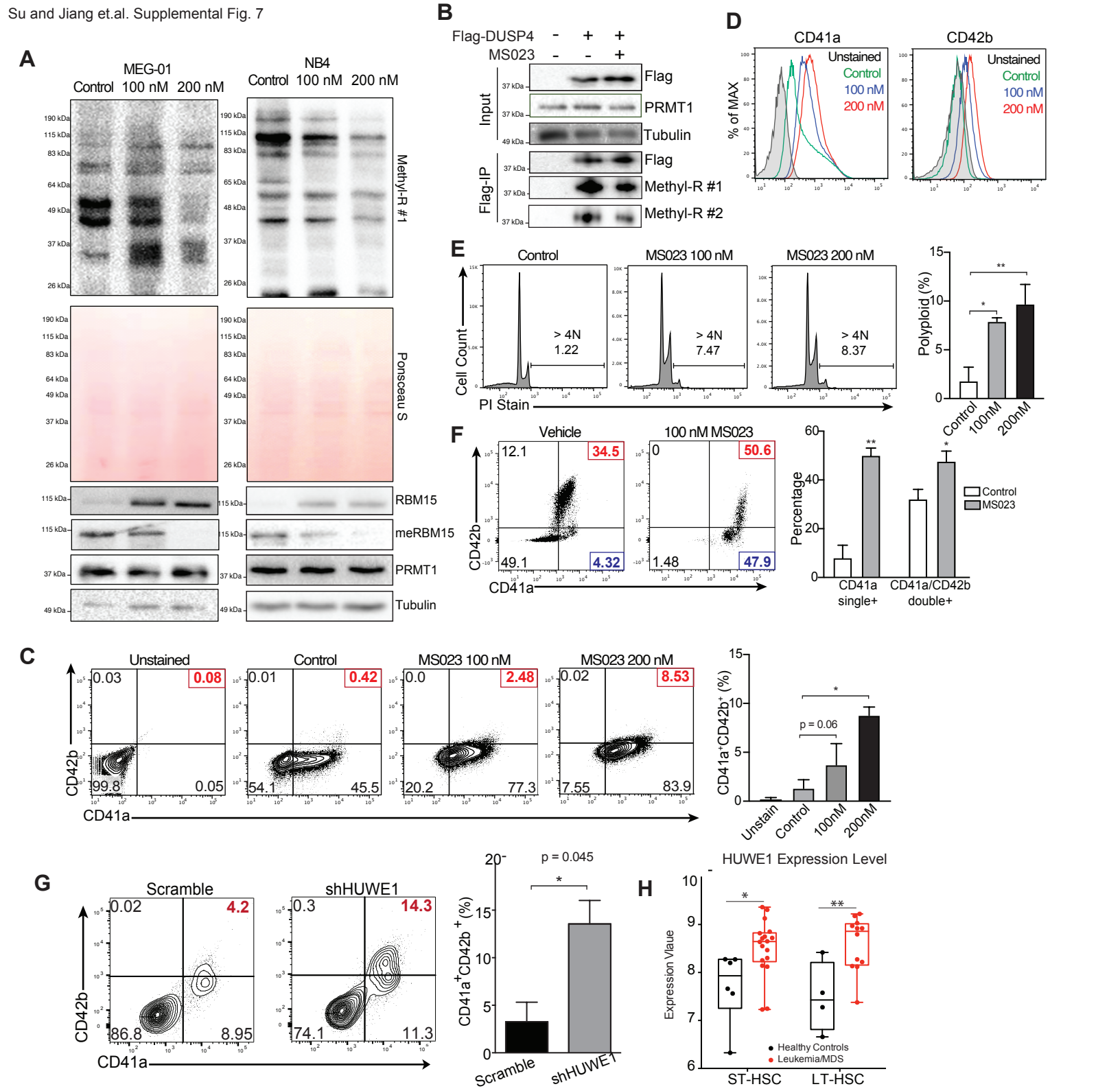

Figure S7. PRMT1 inhibitor MS023 blocks arginine methylation, and both MS023 and HUWE1 knockout enhance Mk differentiation, Related to Figure 7.

(A) Arginine methylation level of MS023-treated cells. MEG01 and NB4 cells were cultured with the presence of control or MS023 for 24 hours. Cell extract was harvested and used for SDS−PAGE. Arginine methylation status was detected by using anti-methyl-R antibody.

(B) Inhibition of DUSP4 methylation by MS023. Flag-tagged DUSP4 was immunoprecipitated from 293T cells treated with MS023. Two generic anti-methyl-arginine antibodies were used for western blotting.

(C) CMK cells were treated with MS023 for 72 hours then stained with anti-CD41a/anti-CD42b antibodies for FACS analysis. Representative plots are shown (n = 2, independent experiments).

(D) Histograms of MS023-treated CMK cells labeled with anti-CD41a and anti-CD42b antibodies, respectively.

(E) Polyploidy of MS023-treated CMK cells were assessed by propidium iodide staining. Cells with DNA content of >4N were counted as polyploidy. Representative plots are shown (n = 3, independent experiments).

(F) Immobilized peripheral CD34+ cells were cultured in Mk-promoting medium (TPO + SCF) with or without the presence of MS023. Cultured cells were harvested on day 7 for FACS analysis. Representative plots are shown (n = 2, independent experiments).

(G) Mk differentiation assays using CD34+ cord blood cells transduced with shRNA agaisnt HUWE1 (n=3, independent experiments). A representative FACS analysis was shown on the left, and the average with STD on the right. (H)Analysis of the HUWE1 gene expression levels in LT-HSC and ST-HSC cells. Results were shown as mean ± SD, two-tailed unpaired t-test, *P ≤ 0.05; **P ≤ 0.01.

Table S1. List of real-time PCR pimrers, related to Method details for real-time PCR analysis:

Name	Sequence
PRMT1-Fwd	5' CCA GTG GAG AAG GTG GAC AT
PRMT1-Rev	5' CTC CCA CCA GTG GAT CTT GT
DUSP4-Fwd	5' AGG CGG CTA TGA GAG GTT TT
DUSP4-Rev	5' CAC TGC CGA GGT AGA GGA AG
HPRT1-Fwd	5' CAC CCT TTC CAA ATC CTC AG
HPRT1-Rev	5' CTC CGT TAT GGC GAC CCG CA

Table S2. List of shRNAs agaisnt DUSPs, related to Figure 1,2 and Figure S1.

SGEP-based	Pelossof et al. 2017; Fellman et al 2013.
Control	shRen.713
shRNA.name	**Antisense.Guide.Sequence**
DUSP1-a	TTATGTAACAAAATGTCTTCTT
DUSP1-b	TTGTATAAAAAAGTCATCCTTA
DUSP2-a	TCTGTATAAATATAAAGTGCTA
DUSP2-b	TTCTGTATAAATATAAAGTGCT
DUSP4-a	TACAACAACGACAACAAAGGGA
DUSP4-b	TATTTCTAGAGGAAGCAGGGAG
DUSP5-a	TTAAAAACAAAAATCACAGTTG
DUSP5-b	TTTTCTTCACATTCACACGGGT
DUSP6-a	TTAGTATTAACCAATTCCGCAC
DUSP6-b	TAAAGAGAAAAAATCATGAGGA
DUSP7-a	TTGAGTGACAGGTTCATCTTCT
DUSP7-b	TAAAAAGTAAACTCAGGTCCGT
DUSP8-a	ATAATATACATTTATAACGGGC
DUSP8-b	TATAATATACATTTATAACGGG
DUSP9-a	AAGAAAGCAACTATGATATGGA
DUSP9-b	TAAATAAACTGTTTATTCAGAA
DUSP10-a	TAAACAAAGGTTGAGATCCTGA
DUSP10-b	TTAATTTGTCAGTTTGTGGGAG
DUSP16-a	TATATTTCAGATTTACAGGGAA
DUSP16-b	ATATATTTCAGATTTACAGGGA
pLKO.1-based	
Control	Scramble
Name	**Sequence**
DUSP4-#1	GCCTACCTGATGATGAAGAAA
DUSP4-#2	CCCAGTGGAAGATAACCACAA
HUWE1	AAACCCAGGGCTGCCTTGGAAAAG

Table S3. Mass spectrometry raw data analysis, related to Figure 5 and Star Methods:

#1	b^{+}	b^{2+}	b^{3+}	Seq.	y^{+}	y^{2+}	y^{3+}	#2
1	157.10840	79.05784	53.04098	R				38
2	244.14043	122.57385	82.05166	S	3925.94648	1963.47688	1309.32034	37
3	357.22450	179.11589	119.74635	I	3838.91445	1919.96086	1280.30967	36
4	470.30857	235.65792	157.44104	I	3725.83038	1863.41883	1242.61498	35
5	557.34060	279.17394	186.45172	S	3612.74631	1806.87679	1204.92029	34
6	654.39337	327.70032	218.80264	P	3525.71428	1763.36078	1175.90961	33
7	768.43630	384.72179	256.81695	N	3428.66151	1714.83439	1143.55869	32
8	915.50472	458.25600	305.83976	F	3314.61858	1657.81293	1105.54438	31
9	1002.53675	501.77201	334.85043	S	3167.55016	1584.27872	1056.52157	30
10	1149.60517	575.30622	383.87324	F	3080.51813	1540.76270	1027.51089	29
11	1280.64567	640.82647	427.55341	M	2933.44971	1467.22849	978.48809	28
12	1337.66714	669.33721	446.56056	G	2802.40921	1401.70824	934.80792	27
13	1465.72572	733.36650	489.24676	Q	2745.38774	1373.19751	915.80076	26
14	1578.80979	789.90853	526.94145	L	2617.32916	1309.16822	873.11457	25
15	1691.89386	846.45057	564.63614	L	2504.24509	1252.62618	835.41988	24
16	1819.95244	910.47986	607.32233	Q	2391.16102	1196.08415	797.72519	23
17	1967.02086	984.01407	656.34514	F	2263.10244	1132.05486	755.03900	22
18	2096.06346	1048.53537	699.35934	E	2116.03402	1058.52065	706.01619	21
19	2183.09549	1092.05138	728.37001	S	1986.99142	993.99935	663.00199	20
20	2311.15407	1156.08067	771.05621	Q	1899.95939	950.48333	633.99131	19
21	2410.22249	1205.61488	804.07901	V	1771.90081	886.45404	591.30512	18
22	2523.30656	1262.15692	841.77370	L	1672.83239	836.91983	558.28231	17
23	2594.34368	1297.67548	865.45274	A	1559.74832	780.37780	520.58762	16
24	2695.39136	1348.19932	899.13530	T	1488.71120	744.85924	496.90858	15
25	2782.42339	1391.71533	928.14598	S	1387.66352	694.33540	463.22602	14
26	2942.45404	1471.73066	981.48953	C-Carbamidomethyl	1300.63149	650.81938	434.21535	13
27	3013.49116	1507.24922	1005.16857	A	1140.60083	570.80405	380.87179	12
28	3084.52828	1542.76778	1028.84761	A	1069.56371	535.28549	357.19275	11
29	3213.57088	1607.28908	1071.86181	E	998.52659	499.76693	333.51371	10
30	3284.60800	1642.80764	1095.54085	A	869.48399	435.24563	290.49951	9
31	3355.64512	1678.32620	1119.21989	A	798.44687	399.72707	266.82047	8
32	3442.67715	1721.84221	1148.23057	S	727.40975	364.20851	243.14143	7
33	3539.72992	1770.36860	1180.58149	P	640.37772	320.69250	214.13076	6
34	3626.76195	1813.88461	1209.59217	S	543.32495	272.16611	181.77983	5
35	3683.78342	1842.39535	1228.59932	G	456.29292	228.65010	152.76916	4
36	3780.83619	1890.92173	1260.95025	P	399.27145	200.13936	133.76200	3

37	3893.92026	1947.46377	1298.64494	L	302.21868	151.61298	101.41108	2
38				R-Methyl	189.13461	95.07094	63.71639	1